Since January 2020 Elsevier has created a COVID-19 resource centre with free information in English and Mandarin on the novel coronavirus COVID-19. The COVID-19 resource centre is hosted on Elsevier Connect, the company's public news and information website.

Sustainable Cities and Society 80 (2022) 103719

Contents lists available at ScienceDirect

Sustainable Cities and Society

journal homepage: www.elsevier.com/locate/scs

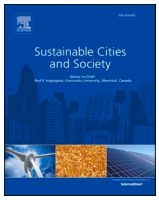

Metabolism-based ventilation monitoring and control method for COVID-19 risk mitigation in gymnasiums and alike places

Junqi Wang [a,b,c], Jingjing Huang [b,d], Qiming Fu [b,d], Enting Gao [b,d], Jianping Chen [b,e,*]

[a] School of Environmental Science and Engineering, Suzhou University of Science and Technology, Suzhou 215009, China
[b] Jiangsu Key Laboratory of Intelligent Building Energy Efficiency, Suzhou, Jiangsu 215009, China
[c] School of Architecture, Southeast University, 2 Sipailou, Nanjing, Jiangsu 210096, China
[d] School of Electronics and Information Engineering, Suzhou University of Science and Technology, Suzhou, Jiangsu 215009, China
[e] School of Architecture and Urban Planning, Suzhou University of Science and Technology, Suzhou, Jiangsu 215009, China

ARTICLE INFO

Keywords:
COVID-19
Ventilation control
Metabolic rate
Healthy society

ABSTRACT

Gymnasiums, fitness rooms and alike places offer exercise services to citizens, which play positive roles in promoting health and enhancing human immunity. Due to the high metabolic rates during exercises, supplying sufficient ventilation in these places is essential and extremely important especially given the risk of infectious respiratory diseases like COVID-19. Traditional ventilation control methods rely on a single CO_2 sensor (often placed at return air duct), which is often difficult to reflect the human metabolic rates accurately, and thus can hardly control the infection risk instantly. Thus, to ensure a safe and healthy environment in places with high metabolism, a real-time metabolism-based ventilation control method is proposed. A computer vision algorithm is developed to monitor human activities (regarding human motion amplitude and speed) and an artificial neural network is established for metabolic prediction. Case studies show that the proposed metabolism-based ventilation control method can reduce the infection probability down to 4.3-6.3% while saving 13% of energy in comparison with the strategy of fixed-fresh-air ventilation. In the development of healthy and sustainable society, gymnasiums and alike exercise places are essential and the proposed ventilation control method is a promising solution to decrease the risk of COVID-19 while preserving features of energy saving and carbon emission reduction.

1. Introduction

Currently, COVID-19 continues to spread globally, with a cumulative death toll of 5.57 million worldwide till January 21, 2022 (World Health Organization (WHO), 2022). In indoor environment, the transmission of COVID-19 includes droplet transmission, contact transmission, and the possibility of aerosol transmission in a relatively closed environment with prolonged exposure to high aerosol concentrations (Noorimotlagh et al., 2021). Ventilation can dilute the concentration of indoor pollutants and reduce the exposure of indoor occupant to pathogens and the risk of infection (Morawska et al., 2020; Ding et al., 2020). The World Health Organization recommends to increase the supply of fresh indoor air as an effective way to reduce the concentration of virus particles in enclosed spaces, thereby reducing the risk of infection. Therefore, effective building ventilation is essential to ensure the health and safety of occupants (Cao et al., 2020a; Kong et al., 2021; Srivastava et al., 2021;).

In high-metabolic-rate venues (e.g., indoor exercise arenas such as gyms, dance studios, boxing studios, etc.), occupants exhale and inhale at much higher rates than in sedentary or office scenarios. The corresponding risks of infection increase exponentially with the metabolic rate. Gymnasiums, as specific places that provide equipment and services for occupant to exercise, are expected to have more significant exhalation and inhalation than in other indoor environments (e.g., office rooms and shopping malls) (Blocken et al., 2021; Blocken et al., 2020). Exhaled droplets may contain pathogens and inhalation may bring pathogens into the human body (Berlanga et al., 2020), which would cause infection. Collective COVID-19 infection cases in gyms have been reported in South Korea (Jang et al., 2020). Data show that the exhalation and inhalation volumes of people in gyms can be 2 times higher than that of a sedentary scenario respectively, which results in a higher rate of infection (Kapalo et al., 2021). Therefore, there is an urgent need

* Corresponding author.
E-mail address: alan@mail.usts.edu.cn (J. Chen).

https://doi.org/10.1016/j.scs.2022.103719
Received 27 December 2021; Received in revised form 23 January 2022; Accepted 25 January 2022
Available online 29 January 2022

to improve ventilation control systems to reduce the risk of respiratory infection. Studies (Monge-Barrio et al., 2022) encouraged using natural ventilation to improve indoor environmental quality. Due to the lack of effective ventilation monitoring and control, the ventilation control in places with high occupant metabolic rates often cannot satisfy the requirement of infection prevention during COVID-19 outbreak. Stadiums, gyms and alike places (with high metabolism) play an important role in society considering the health and well-being of people. Traditional CO_2 based ventilation control relies on the single CO_2 sensor that is commonly placed at return air duct. It cannot reflect the CO_2 distribution correctly and has time delay due to the air mixing process (Cakyova et al., 2021; Shin et al., 2018). Thus, the traditional CO_2 based ventilation cannot control the risk of infection satisfactorily.

Therefore, to ensure the safe operation of gyms, stadiums, and alike places in the post-epidemic era, it is of great importance to provide reasonable online occupant monitoring and ventilation control methods for venues with high occupant metabolic rates. Recent studies have shown that information based on occupant monitoring can be used to predict ventilation requirement and thus perform controls such as demand controlled ventilation and energy conservation (Cao et al., 2020b). For example, Jin et al. (2018) proposed a ventilation control strategy based on occupant information with an energy savings potential of 55% for the ventilation system. Pang et al. (2020) demonstrated simulation experiments using the number of people as a key control factor, which can effectively reduce building energy consumption by 25-40%. Wang et al. (2021) proposed an intelligent ventilation strategy that provides fresh air volume based on real-time occupant density, which can reduce the risk of infection to less than 2% to some extent while saving 11.7% of energy at the same time. Mokhtari and Jahangir (2021) proposed a ventilation strategy based on occupant distribution that could reduce the number of infections by 56% and energy consumption by 32%. Morawska et al. (2021) pointed out that future ventilation systems should vary the ventilation air rate in different places depending on the activity, and thus reducing the risk of indoor respiratory disease infections. However, there is a lack of studies investigating occupant metabolic rate monitoring and the corresponding ventilation control system.

The accurate monitoring of metabolic rate requires expensive professional instruments and equipment (e.g., the measurement equipment-MED K5 used by Yang et al. (2021)). With the development of modern technology, new instruments and methods of metabolic rate measurement have emerged. Scholars have tried to use wearable devices, such as smart bracelets (H. Na et al., 2020; Hasan et al., 2016; Nagarajan et al., 2021), to monitor the metabolic rate. However, not everyone wears a smart bracelet in daily life. Kinect camera (H. S. Na et al., 2019) and passive infrared thermal imaging sensors (Enis Cetin et al., 2021) were also used to monitor and predict human metabolic rate, but they are not widely used in buildings. As a result, the above-mentioned methods of obtaining metabolic rate require additional cost of equipment.

In recent years, computer vision technology has been widely used in occupant detection given its rapid development and advantages. Computer vision simulates the human visual system by analyzing the rich information provided by digital images or video to achieve a high level of understanding of objects and events presented in a scene (Guo et al., 2021). Using traditional surveillance cameras, computer vision technology can obtain information about occupants at a low cost, such as occupant number (Wang et al., 2019), density (Sun et al., 2022; Wang et al., 2018), location (Huang & Hao, 2020), and posture (Chun et al., 2015). This paper combines computer vision techniques and artificial neural network to predict metabolic rates which are used as the input signal for ventilation control to reduce the risk of respiratory infection. A case study is conducted to evaluate the energy performance and infection probability of the proposed metabolism-based ventilation control method.

2. Methodology

2.1. Overview of the study

The method of the proposed metabolism-based ventilation control is shown in Fig. 1. Firstly, cameras are used to acquire videos and computer vision algorithm is used to obtain human activity related features. Then, a constructed prediction model is used to output the metabolic rate for the final ventilation control.

The detailed framework diagram is shown in Fig. 2, which consists of (a) metabolic rate prediction and (b) ventilation control and assessment. Based on the video acquired from surveillance cameras, this method extracts two indicators to reflect the occupants' activity intensity, which are used in the metabolic rate prediction. Then, metabolic rate and generation of CO_2 are input to equation, which are used to estimate the ventilation rate. Finally, energy consumption, infection probability and carbon emission are evaluated.

The detailed process is as follows:

(a) Model development: this part is aimed to develop a model to predict metabolic rate. Video from camera is captured firstly, then the background subtraction algorithm is used to process video. After this, the foreground pixel that represents occupant information is obtained, from which the center coordinates of occupant are estimated. To get the moving speed in the real physical world, an artificial neural network model (named ANN_D) is constructed to correct the physical distance based on the image information. At the same time, the Exclusive-OR operation is performed based on background subtracted image frames to obtain the motion amplitude information of occupants. After extracting features of moving speed and motion amplitude from the frames, an artificial neural network model called ANN_M is used to predict metabolic rate. Besides, metabolic rate of occupant is also cross-validated by heart rate measurement acquiring from smart bracelets.

(b) Ventilation control and assessment: the metabolic rate predictions and generation of CO_2 were determining factors of ventilation rate. Finally, the ventilation energy consumption, infection probability and carbon emission are evaluated.

2.2. Image processing: Background subtraction algorithm

The background subtraction algorithm uses the Adaptive Gaussian Mixture Model (AGMM) algorithm, where the white-pixel represents the foreground and the black-pixel represents the background in images obtained after algorithm processing.

AGMM algorithm updates the parameters and the number of Gaussian components for each pixel. The algorithm is able to adapt to changes of background settings (e.g. furniture), so as to minimize the impact of human intervention. Another merit is the ability to adapt to sudden changes of illumination. For example, the user may turn off some lights when watching videos, which would result in peak dropping of foreground pixel. AGMM can be expressed as follows: Eq. (1) is used to determine whether a pixel (D) belongs to the foreground (FG) or background (BG).

$$\mathrm{D} = \frac{p\left(BG|x_{(t)}\right)}{p\left(FG|x_{(t)}\right)} = \frac{p\left(x_{(t)}|BG\right)p(BG)}{p\left(x_{(t)}|FG\right)p(FG)} \tag{1}$$

Where $x_{(t)}$ is the value of pixel in color space (e.g., RGB) at time t. Since the information of FG objects is unpredictable, it is assumed that the FG objects are a uniform distribution, i.e., $p(x_{(t)}|FG) = c$. The BG model is estimated from the training set Kand the training set K is denoted as $\mathrm{p}(x|K, BG)$. To accommodate the background changes, the time interval is set as T, and the training set is $K_{\mathrm{T}} = \{x_{(t)}, \ldots, x_{(t-\mathrm{T})}\}$. For each new sample, the K_{T} is updated. Since the samples may contain FG, the probability density is estimated by the Gaussian Mixture Model (with M group components) is estimated. The output figure is shown in Fig. 3 (b).

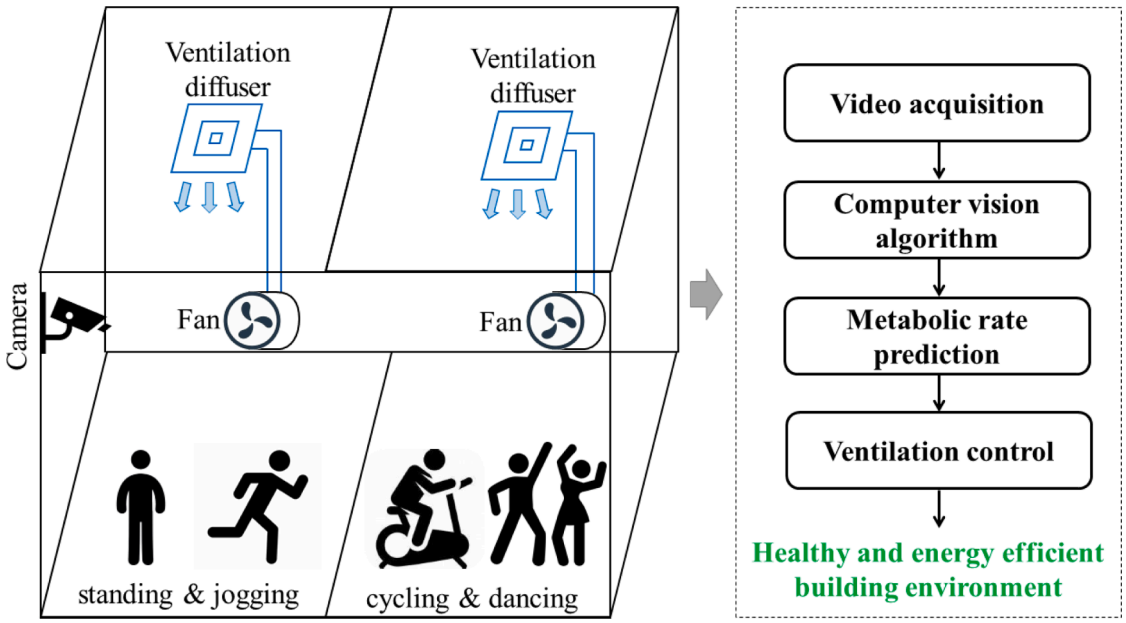

Fig. 1. The metabolism-based ventilation control

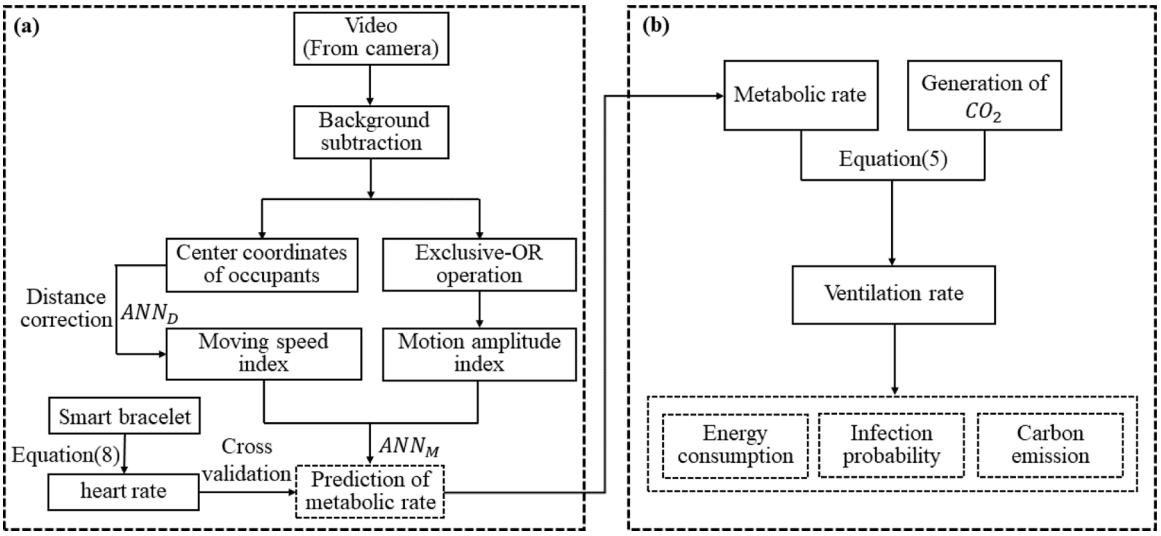

Fig. 2. Framework diagram: (a) metabolic rate prediction (model development) (b)ventilation control and assessment

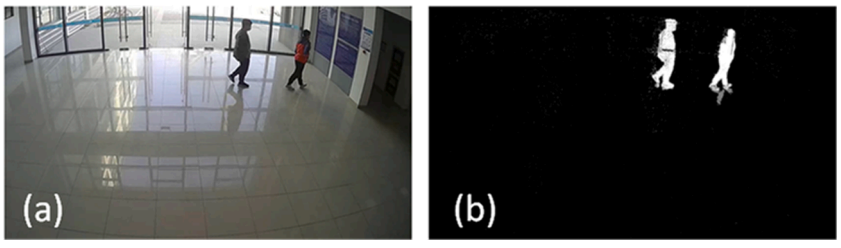

Fig. 3. (a) original image; (b) output image of background subtraction

$$p(x|N_T, BG+FG) = \sum_{m=1}^{M} \hat{\pi}_m N\left(x; \hat{\mu}_m, \hat{\sigma}_m{}^2 I\right) \quad (2)$$

where $\hat{\mu}_m$ is the estimate of the mean of the Gaussian component, and $\hat{\sigma}_m{}^2$ is the estimate of the variance of the Gaussian component, and I is the unit matrix, and $\hat{\pi}_m$ is the estimate of the mixture weights ($\hat{\pi}_m \geq 0, \sum \hat{\pi}_m = 1$).

The AGMM algorithm consists of three steps:

(1) Use the following formula for the new sample $x_{(t)}$ to classify: $p(x_{(t)}|N_T, BG) > \delta$
(2) Update: $p(x|K_T, BG + FG)$

(3) Update: $p(x|K_T, BG)$

where (δ is to determine $x_{(t)}$ whether it belongs to the threshold of BG.)

2.3. Metabolic rate prediction model

2.3.1. Motion amplitude index

The pixel value, which is denoted as $P_{(X,Y)}$ in frame I(X, Y) is represented by 0 or 255, where 0 means white-pixel and 255 means black-pixel. Comparing the value of the pixel at all locations of the adjacent frame, and the number of pixel points with an Exclusive-OR operation value of 1 is counted as N_I, which is used to represent the degree of motion amplitude of occupants.

2.3.2. Moving speed index and physical distance correction model

In the coordinate system of image, the horizontal and vertical coordinates of all white-pixel in frame I are averaged to obtain with X_i and Y_i, which are the location of the occupant center point coordinates $M(X_i, Y_i)$, and the center point of occupant in the adjacent frame (I-1) is selected as $M'(X_{i-1}, Y_{i-1})$. The Euclidean distance between $M(X_i, Y_i)$, and $M'(X_{i-1}, Y_{i-1})$ indicates the moving distance D_i of the occupant.

$$D_i = \sqrt{(X_i - X_{i-1})^2 + (Y_i - Y_{i-1})^2} \tag{3}$$

The occupant movement speed in the physical coordinate system is estimated by Eq. (4), where T represents the sampling time that indicates the time difference between two adjacent frames.

$$v_I = D_I / T \tag{4}$$

$$D_I = f_{ANN_D}(D_i,\ M(X_i, Y_i),\ M'(X_{i-1}, Y_{i-1})) \tag{5}$$

Since the image coordinates and real physical coordinates are different, it is essential to correct the moving speed index v_i. Specifically, the image coordinate system uses the left-up corner as the original point, while the physical coordinate system uses the left-bottom corner as the original point (see Fig. 4). To correct the physical distance D_i, $M(X_i, Y_i)$, $M'(X_{i-1}, Y_{i-1})$ and D_i are used as the inputs of the artificial neural network model ANN_D, and the physical distance of the occupant in the adjacent frame is taken as the output (represented in equation(5)). The physical distance correction process is shown in Fig. 4. The relationship between the image coordinate system and the real physical coordinate system is obtained by the Neural Net Fitting regression in MATLAB toolbox, so as to obtain the real moving speed of the occupant.

2.2.3. Occupant metabolic rate prediction model

The occupant metabolic rate prediction model is implemented by an artificial neural network ANN_M, consisting of two input neurons, two hidden neurons and one output. In which the movement amplitude index N_I and movement speed index v_I are the inputs of ANN_M, and the real metabolic rate of the person as the output M. The prediction model is finally obtained by fitting the Neural Net Fitting regression in MATLAB toolbox.

2.2.4. Ventilation rate based on metabolic rate

Metabolism-based ventilation rate estimation:

The rate of occupant's CO_2 generation emanation is used to indicates the human metabolic rate, so the dilution of occupant's CO_2 emanation is used to determine the minimum amount of fresh air required by occupant can be estimated by Eq. (6).

$$v = g/(c - c_o) \tag{6}$$

$$g = 4\ \times 10^{-5}(MA_P) \tag{7}$$

Where v denotes the amount of fresh air every occupant required to dilution CO_2, and c denotes the allowable indoor CO_2 concentration, and c_o indicates the outdoor CO_2 concentration. g denotes the CO_2 generation rate per person (L/s), which can be calculated from Eq. (7) (China Academy of Building Science, 2016) where M denotes the metabolic rate (W/m^2), A_P denotes the surface area of the body (m^2).

Metabolic rate model validation:

For the validation of metabolic rate model, the human metabolic rate is also calculated based on the heart rate value by Eq. (8) (Nishi, 1981).

$$M_i = \frac{21(0.23RQ + 0.77)Q_{O_2}}{A_D} \tag{8}$$

Where RQ denotes the respiratory quotient (dimensionless), and Q_{O_2} represents the volumetric rate of oxygen consumption (mL/s) at certain conditions (obtained based on heart rate estimation), and A_D denotes the surface area of the body (m^2). The relationship between oxygen consumption and heart rate of a person under different intensity of exercise is shown in Table 1.

2.4. Ventilation performance evaluation

2.4.1. Ventilation energy consumption

The energy consumption of ventilation system includes two parts: air conditioning consumption and fan operation consumption. Air conditioning system consumption can be calculated by Eq. (9):

$$P_{fresh} = Q/COP \tag{9}$$

Where Q indicates the ventilation load (W) that can be obtained from Eq. (10), and COP indicates the coefficient of performance of the chiller

Table 1
Heart rate and oxygen consumption at different activity level (Astrand and Rodahl, 1977)

Level of Activity	Heart rate (Beat per Minute)	Oxygen consumption (mL/s)
Light work	<90	<8
Moderate work	90~110	8~16
Heavy work	110~130	16~24
Very heavy work	130~150	24~32
Extremely heavy work	150~170	>32

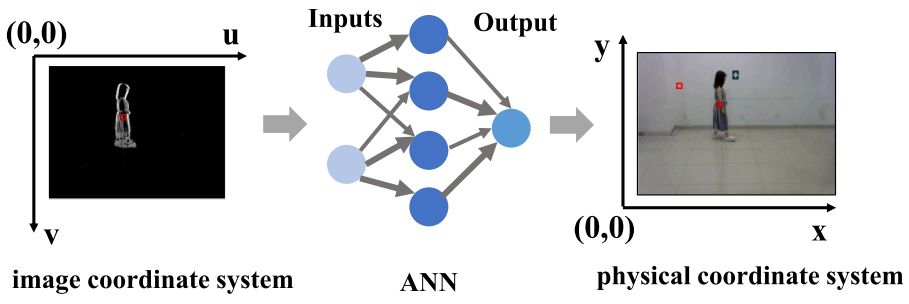

Fig. 4. Physical distance correction process

plant.

$$Q = V_0 C_P (t_R - t_O) \tag{10}$$

V_0 indicates the fresh air volume (kg/m^3);C_P denotes the specific heat of air at constant pressure; t_R and t_O represent the design indoor and outdoor temperature of air conditioning in winter (the experiment of energy consumption was conducted in winter), respectively. The energy consumption of the fan (kW) can be calculated by Eq. (11).

$$P_{fan} = \beta F^3 \tag{11}$$

Where F indicates the air flow rate (m^3/s), β denotes the coefficient.

In this study, the proposed ventilation strategy based on occupant metabolic rate is compared with the traditional fixed fresh air strategy and the ventilation strategy based on the number of occupants.

strategy (1): fixed fresh air

This strategy sets the fresh air delivery volume to a fixed ratio (e.g., 15-30%), and this study provides fresh air ratio based on room size with full occupancy.

strategy (2): based on the occupant number

This strategy takes the density of occupant as the main reference and supplies the ventilation rate according to the demand of occupant. The amount of fresh air required for each person follows the recommended values in the ventilation standard (China Academy of Building Science, 2016).

strategy (3): based on the occupant metabolic rate

The total metabolic rate of occupants is acquired by taking the metabolic rate and CO_2 generation of occupants into account, and metabolic rate is predicted by the model ANN_M. The required ventilation rate is estimated based on the CO_2 generation rate and the required CO_2 concentration (see Eq. (6)).

2.4.2. Probability of infection

The Wells-Riley model is used for the assessment of infection risk, which is one of the most classic and popular models for predicting infection risk. To make the calculation of infection rate more accurate, the Wells-Riley model is modified as shown in the following formulas (Sun & Zhai, 2020):

$$P_I = \frac{C}{S} = 1 - \exp\left(- P_d \frac{Bqpt)}{E_Z Q/N} \right) \tag{12}$$

$$P_d = (-18.19\ln(d) + 43.276)/100 \tag{13}$$

Where P_I is the infection probability; C is the number of patients who are infected; S is the total number of susceptible patients; I is the number of infections represented; and B represents the probability of initial infection; p denotes the respiratory volume (m^3/s); Q *is the* room ventilation rate (m^3/s), q represents the dose at which infectious particles occur; t is the exposure time (s); E_z is the efficiency of air distribution in space; and d is the social distance; N represents the number of occupants.

2.4.3. Carbon emissions

The carbon emission is also calculated, which consists of electricity consumption from ventilation (U_{fan}) and hospital treatment caused by COVID-19 infection ($U_{treatment}$). Electricity is the main source of carbon emission in this study, which can be calculated with Eq. (14):

$$C = EF \times \left(U_{fan} + U_{treatment} \right) \tag{14}$$

Where EF denotes the grid emission coefficient, U represents energy consumption of electricity (kWh). $U_{treatment}$ is calculated by the energy consumption of hospital treatment multiplied the infection probability (Eq. (12)).

3. Case study

3.1. Experimental environment

This experiment was conducted in a laboratory of a university. As shown in Fig. 5, the video capture area with 6m (length) ×4.5m (width) ×5m (height), the room temperature was controlled at 24°C ± 0.5°C, and the relative humidity was maintained at 40%-70%. The red star in the Fig. 5 is the test points of indoor temperature and humidity. Logitech C505e camera was used to capture video, and a smart bracelet (model type: XMSH11HM) was used to detect heart rate. The camera is installed at a height of 2.6 meters above the ground to capture as much of the interior as possible.

Before the experiment, the subjects would sit still for 15 minutes to minimize the influence of external factors on the subjects' physiology and psychology.

Experiment 1 was designed to predict the metabolic rate of occupant. The subjects performed three exercises sequentially: standing to relax, jogging and running, each exercise lasting 5 minutes, with an interval of 15 minutes between different exercises, during which they wore a smart bracelet to detect their heart rate in real time, with a sampling frequency of once per minute (to verify the accuracy of metabolic rate prediction), and the process is shown in Fig. 6.

Experiment 2 (18:00~18:10 on November 15 of 2021) recorded the video of two occupants performing 10 minutes of fitness exercise, which was used to evaluate the ventilation performance of the three ventilation strategies. The subjects' information is listed in Table 2.

The metabolic rate prediction model and ventilation rate calculation codes are embedded in the micro controller unit. When the camera captures occupants, the micro controller unit calculates the metabolic rate of the occupants based on the proposed method, and then calculates the ventilation rate required by the occupants in real time. Finally, the micro controller unit outputs control signals to a digital-to-analogue converter which can adjust the fan speed by changing the output voltage. The detailed control schematic is shown in Fig. 7.

3.2. Parameter settings

The estimated metabolic rate value is used as the ground truth to develop the metabolic rate model of the ANN_M, while the predicted metabolic rate is the basis for controlling the fresh air volume in the ventilation system. The parameters in Eq. (8) take the following values: RQ is set as 0.83 for light and sedentary work (Nishi, 1981); A_D is selected as 1.69m^2;Based on the measured heart rate, Q_{O_2} is estimated with Table 1.

The Wells-Riley equation is used to calculate the infection probability and the values of the parameters are set as following: d is selected as 2 m which is a generally recommended social distance in public venues (Wang et al., 2021), so P_d is set as 0.359; B is set as 2.2% based on previous cases (Wang et al., 2021); q is the quantum generation rate and is selected as 0.0394 quantum/s (142 quantum/h) (Buonanno et al., 2020); p is set as 8.28L/min based on the level of activities. Exposure time t is selected as 600s (i.e., 10 mins of experiment). Q represents the fresh air volume, which is calculated based on the metabolic rate of the occupants. E_Z is set as 1 in this case study (Wang et al., 2021). In the calculation of ventilation energy consumption, COP is set as 4.2; β is set as 0.8, according to a catalogue of fan; C_P is selected as 1.005kJ/(kg·C); t_R and t_O is set to 22°C and -2.5°C, respectively (China Academy of Building Science, 2016).

Carbon emissions is calculated by Eq. (14) and the parameters use the following values: EF is set to 0.7921 (Ministry of Ecology and Environment of the People's Republic of China, 2019); Based on the investigation of 30 hospitals in China (Shi et al., 2021), the average energy consumption is set to 180 kWh/(m^2•a). Assuming each patient accounts for 12 m^2 of inpatient ward, the energy consumption for one

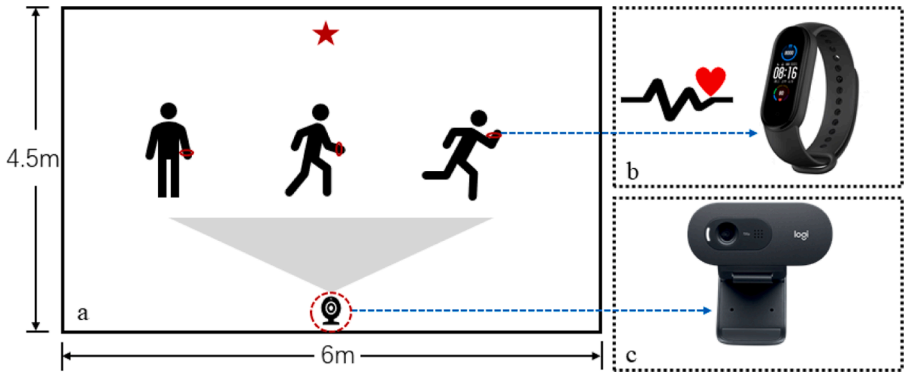

Fig. 5. (a) experimental scenario (b) heart rate monitoring bracelet (c) camera

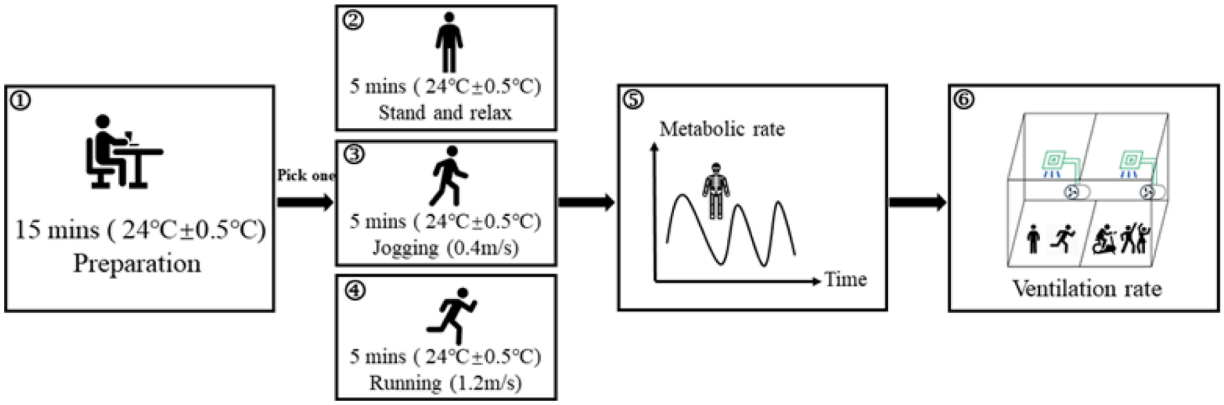

Fig. 6. Flow diagram of experiment

Table 2
Basic information of subjects

Occupant	Gender	Age (years old)	Height(cm)	Weight(kg)
A	Male	23	170	68
B	Male	23	176	69

people in hospital is 3.95 kWh/day (or 3.12 kg/day carbon emission per people). Note that the calculation duration of carbon emission is set to 10 minutes to align with the experiment.

3.3. Results

3.3.1. Motion amplitude index and movement speed index

The original video was intercepted frame by frame after background subtraction processing, and every three frames were sampled once. The

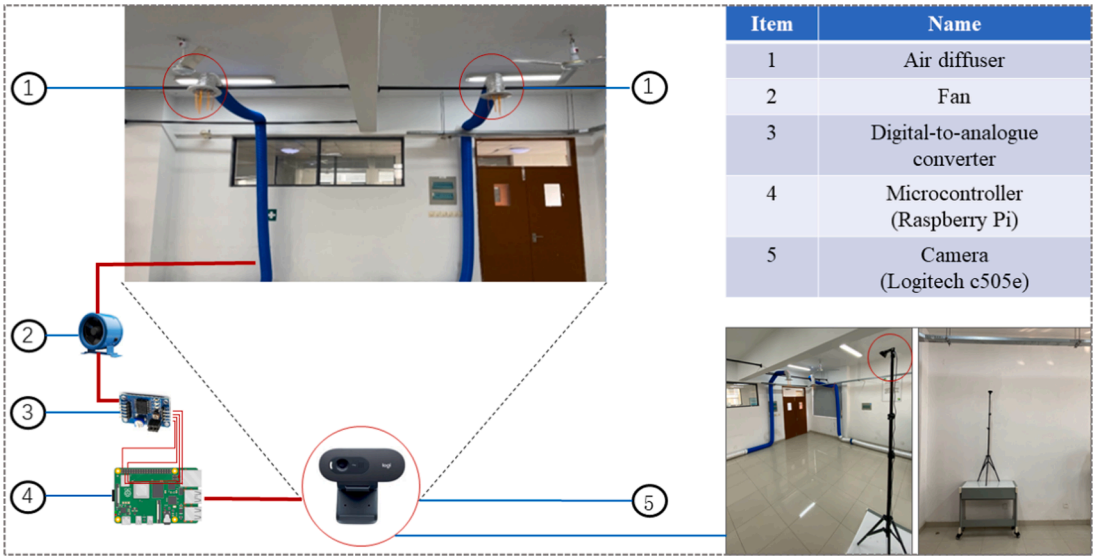

Item	Name
1	Air diffuser
2	Fan
3	Digital-to-analogue converter
4	Microcontroller (Raspberry Pi)
5	Camera (Logitech c505e)

Fig. 7. The control schematic and experimental scenes

adjacent frames in the new set of sampled frames are subjected to the Exclusive-OR operation to obtain the contour of the occupant's motion magnitude as shown in Fig. 8, and the number of white-pixel in the frame is counted (N_I), which is positively related to the magnitude of occupant motion. The results show that: in the standing state, the movement of occupant is not obvious and the outline of the occupant is faint; the faster the walking speed at the same sampling interval, the sharper the outline of occupant is, namely, the larger the proportion of the number of white-pixel in the whole picture.

Occupant moving speed is another input parameter of metabolic rate prediction model, which needs to be corrected based the real physical distance of occupant movement. Based on the data collected in Experiment 1, the artificial neural network ANN_D was established with 1800 sample images. Among these images, 70% was for training, 15% was used to test and the last 15% was for validation. At last, the model acquired a R value (regression value) of 0.9675 (shown in Fig. 9). Thus, the physical correction model ANN_D is feasible to be used in this case study.

3.3.2. Occupant metabolic rate prediction

A recorded video with thirty minutes was used to verify the accuracy of the occupant metabolic rate prediction model. During the experiment, occupants were in standing to relaxing, jogging and running states (lasted ten minutes for each activity). Each occupant wore a bracelet and the heart rate was measured every two minutes. The occupant metabolic rate can be monitored in real time by the smart bracelet and substituted into Eq. (8), and the real value of occupant metabolic rate is shown in Fig. 10(a). Take jogging as an example, the occupant metabolic rate gradually rises from 144W, reaches 168W and then gradually falls back to 156W, and generally stays around 156W, during which the occupant metabolic rate shows a dynamic change with a smooth overall trend. Through the formula $|\frac{TR-TP}{TR}| \times 100\%$ (TR represents the ground truth of metabolic rate that was measured, and TP represents the predicted metabolic rate), the prediction error rate of the occupant metabolic rate is computed as 8.9% (meaning a 91.1% accuracy), which is acceptable in engineering applications.

3.3.3. Ventilation strategy evaluation

The effectiveness of the proposed metabolism-based ventilation control was verified by a comparative experiment. The scenario is shown in Fig. 5 (a) with two occupants exercising at high intensity. In this experiment, fixed fresh air ventilation is used as the benchmark for comparison of energy saving and infection probability. According to the building ventilation design guideline, the required fresh air volume for occupant in gym premises is 60 $m^3 \cdot (h \cdot p)^{-1}$. The density of occupant is 0.2 person/m^2 (China Academy of Building Science, 2016), and the room size is 6m(length) $\times$ 4.5m(width) $\times$ 4m(height). Thus, the full occupancy is 6 occupants. For the fixed fresh air ventilation strategy, the fresh air volume is given according to the full occupancy (i.e., 360 m^3/h). The occupant-number-based ventilation strategy provides the fresh air according to the actual occupant number (namely two in this case), so the total fresh air volume is 120 m^3/h. For the metabolism-based ventilation strategy, the required fresh air volume is calculated by substituting metabolic rates into Eq. (6) and Eq. (7), which gives an average ventilation rate of 313 m^3/h.

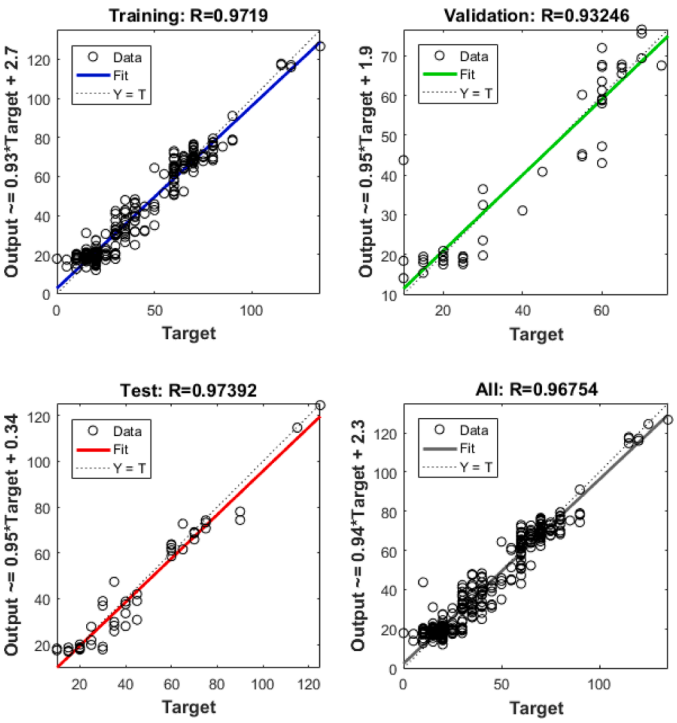

Fig. 9. Regression of correcting distance

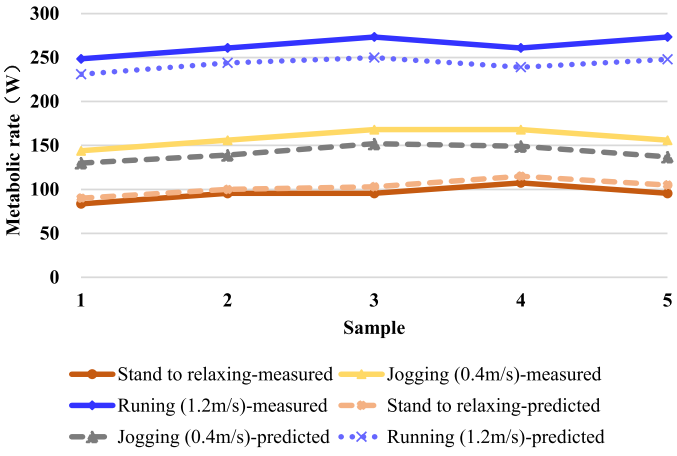

Fig. 10. Occupants' metabolic rates in different states: measured and predicted values

The infection probabilities under different ventilation strategies can be calculated based on Eq. (12), and the results are shown in Fig. 11 and

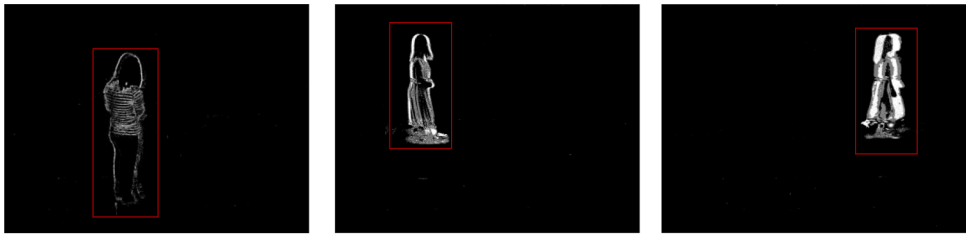

(a) Standing (0m/s) (b) Walking (0.4m/s) (c) Walking (1.2m/s)

Fig. 8. Plots of motion amplitude under different motion types

Table 3. The infection probability is 4.3% under the fixed fresh air ventilation strategy (denoted as "S1"), and up to 12.4% at full occupants. The occupant-number-based ventilation strategy (denoted as "S2") has an infection probability of 12.4% all the time, which is the highest. The metabolism-based ventilation strategy (denoted as "S3") can control the infection probability to the range of 4.3-6.3% with an averaged infection probability of 5.0%. Regarding the energy performance, S1 is set as the benchmark. By calculation, S2 can save 66% of energy but the infection probability is out of control. S3 can save 13% energy consumption, while maintaining a relatively low infection probability. For the carbon emission, S2 achieves the lowest emission, but it can not effectively control the infection probability. Comparing with S1, the proposed S3 offers a lower carbon emission, which provides a more sustainable way for ventilation control in gym and alike places.

As the epidemic enters into the regular management, ventilation control in public places should not be neglected, especially in places with high metabolic rate of occupant. It is more important to provide ventilation that matches the metabolic rate of occupants to minimize the risk of indoor transmission of respiratory infections. Traditional ventilation control methods would use a design maximum ventilation rate all the time, but may consume unnecessary energy at a low occupancy. The proposed metabolism-based ventilation control can achieve an equivalent infection probability and enable a demand-controlled feature that can effectively save energy.

(Note: "Vent. Rate" – Ventilation Rate; "IP" – Infection Probability; "S1": fixed fresh air ventilation strategy; "S2": occupant-number-based ventilation strategy; "S3": metabolism-based ventilation strategy)

4. Discussions

Engineering implications

Public buildings, gymnasiums and alike exercise places are essential to promote the human heath and wellbeing since regular exercise has a positive and profound influence on the human immune system (Simpson et al., 2015; Ibrahim & Hassanain, 2022). However, due to the quarantine and lockdown in COVID-19 outbreak, the physical exercise activities have been decreasing. In the modern society and cities, indoor sport venues are still important due to the severe outdoor air pollution (e.g., traffic pollution and haze) (Zhao et al., 2021), while the infection risk is significant in these places considering the high human metabolic rates. Therefore, innovative ventilation strategies are needed to create a heathy indoor environment and promote physical fitness in a safe way (Cao et al., 2021; Panaras et al., 2018). The proposed metabolism-based ventilation control method is promising to decrease the risk of COVID-19 in indoor sport places while preserving an energy saving feature, which is of great importance towards the development of healthy and sustainable society. Moreover, the implementation cost is also low since the realization of computer vision algorithm and ventilation control only require a low-cost micro controller (Wang et al., 2021).

In addition, human metabolic rate is one of the most important factors affecting occupant thermal comfort (Pan et al., 2020). Calvaresi et al. (2018) used the real-time measured human metabolic rate to optimize the thermal comfort model, and the results showed that occupant comfort can be improved and building energy management is optimized comparing with the ventilation volume with fixed metabolic rate. Thus, the metabolic rate prediction modeling method proposed in this paper cannot only be used for control of ventilation, but also be utilized in thermal comfort prediction, ventilation demand prediction (Ren & Cao, 2020), and control of thermal comfort (Shan et al., 2020). It should be noted that the procedure developed in this study can calculate the metabolic rate of multiple occupants recorded in one camera. Since the metabolic rate can be added together, the total ventilation rates of multiple occupants can be obtained accordingly. To fulfill this purpose, an occupant identification function is needed to identify the moving speed of different occupants.

Motion amplitude index and moving speed index

The occupant metabolic rate refers to the heat generated per unit of body surface area per unit of time, and is closely related to the intensity of the occupant's activity. The degree of movement amplitude, as one of the indicators of the intensity of occupant activity, reflects the magnitude of the occupant's movement during exercise. When occupant move at a faster speed, the image obtained by the Exclusive-OR operation has less overlapping part of occupant compared with the jogging case. As shown in Fig. 8(b) and (c), the number of white pixels in the foreground

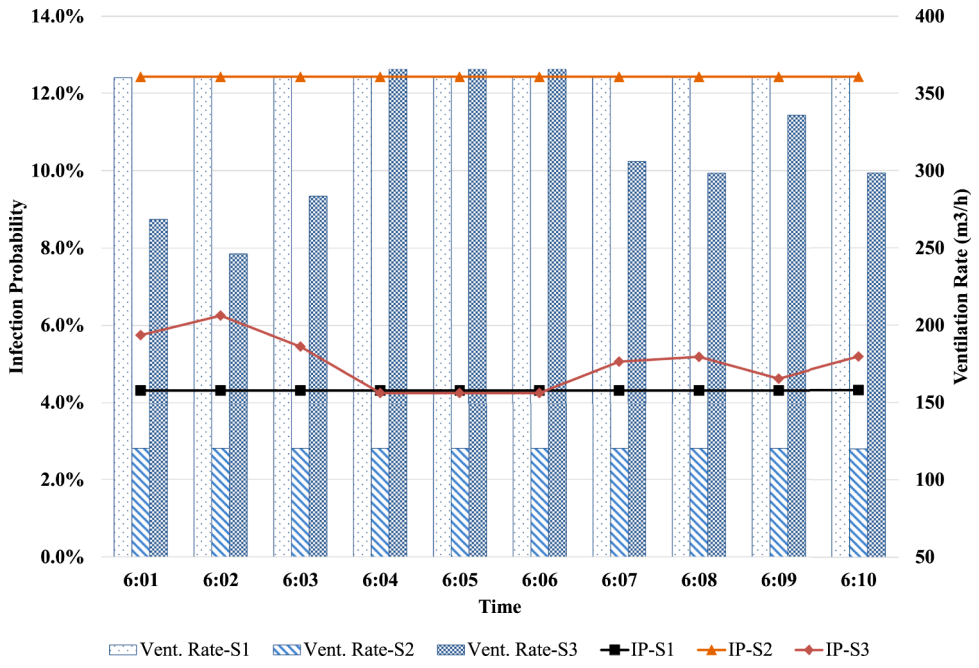

Fig. 11. Infection probabilities and ventilation rates of three ventilation strategies

of the person in the image rises sharply when the person is walking at a speed of 1.2m/s, indicating that the Exclusive-OR operation can effectively reflect the magnitude of the occupant's activity. For the exercise spaces like gyms, the types of people's activities are generally sitting, standing, walking and running. Based on the results, the Exclusive-OR operation is promising to reflect motion amplitudes in most of the activities. It should be noted that weight exercises may not be notably reflected in terms of motion amplitude. However, weight exercises could have extremely high metallic rate. This should be further investigated in our future study.

The human metabolic rate can be determined based on the activity status of the person (mainly deduced from the speed of movement and type of activity). Kang et al. (Kang et al., 2012) estimated occupant metabolic rate by body movement acceleration, which can be used without disturbing the normal activities of the subjects. Therefore, it is reasonable to use occupant moving speed as one of the indicators of occupant activity intensity.

For the video processing, sampling time affects the extraction results of the two indexes. For example, when choosing a longer sampling time, the motion amplitude index can hardly catch the occupants' transient motion. On the contrary, a shorter sampling time will make the real distance hard to compute because the occupants' real moving distance between adjacent images would be very small, bringing more errors into the index of moving speed. Thus, it is critical to choose a suitable sampling time.

Limitations

This paper focus on the monitoring of occupant metabolic rate and control the ventilation accordingly to reduce the risk of indoor transmission of respiratory infections. However, there are several limitations: (1) the indicators used to predict the metabolic rate of occupant and the number of samples required for model prediction need to be further enriched to enhance the accuracy and applicability of the prediction model (e.g., expand the training data to cover weight exercises with light motion amplitude but high metabolism); (2) the regression model varies with the camera angle and scenario, and the prediction model needs to be tailored for the corresponding scene; (3) the experimental case study has a limited occupancy and an actual gym case with large occupancy will be conducted in the future; (4) the study only considers ventilation control, while air disinfection technology can be coordinated in the future (Feng, Cao, & Haghighat, 2021; Feng, Cao, Wang, Kumar, & Haghighat, 2021).

5. Conclusions

Gymnasiums, fitness rooms and alike places offer important exercise services to citizens, which play positive roles in promoting physical fitness and enhancing immunity of human. Due to the high metabolic rates during exercises, supplying sufficient ventilation in these places is essential to ensure a safe indoor environment considering the risk of infectious respiratory diseases like COVID-19. However, traditional ventilation control methods fail to monitor the dynamic metabolic rates and respond to the corresponding ventilation demands. Thus, this paper proposes an innovative method to monitor occupant metabolic rate based on computer vision algorithms in real-time and use occupant metabolic rate for ventilation control. Following conclusions are obtained:

Two indices, motion amplitude index and moving speed index, are developed based on image features and are found to be suitable in reflecting human metabolic levels. The artificial neural network based metabolic prediction model achieves an accuracy of 91.1%, which is acceptable in engineering applications.

The fixed fresh air ventilation strategy can control the infection probability to 4.3% with the designed maximum ventilation supply but has a high energy consumption. The occupant-number-based ventilation strategy has the highest infection probability of 12.4% since it does not consider the human metabolic rate. In comparison, the proposed metabolism-based ventilation control can maintain an equivalent infection probability (4.3-6.3%) and offer an effective energy saving (13% compared with fixed fresh air ventilation strategy).

Table 3
Performance evaluation of three ventilation strategies

Ventilation strategy	Energy consumption (Wh)	Carbon emission (kg)	Energy saving rate	Infection probability
Fixed fresh air	127	0.132	/	4.3%
Occupant-number-based ventilation	43	0.102	66%	12.4%
Metabolism-based ventilation	111	0.122	13%	5.0%

It should be noted that the used computer vision algorithm has a good privacy protection since the foreground objects (e.g., occupants) are subtracted from the background and represented in purely white pixels. In addition, the proposed ventilation control method is low-cost and has a good applicability not only in ventilation but also in thermal comfort applications. As the proposed metabolism-based ventilation strategy achieves an excellent balance between energy consumption, risk mitigation of infection probability and cost, it offers a promising and sustainable solution to decrease the risk of COVID-19 and alike respiratory diseases in places with high occupant metabolism (e.g. gyms and similar sports buildings). More importantly, the design and operation of future sport buildings should be occupant-oriented throughout its whole life cycle and economic precautionary measures (e.g., smart ventilation and air disinfection technologies) should be established in post-pandemic era.

Conflict of interest statement

The authors declared that they have no conflicts of interest to this manuscript. We declare that we have no financial and personal relationships with other people or organizations that can inappropriately influence our work, there is no professional or other personal interest of any nature or kind in any product, service and/or company that could be construed as influencing the position presented in, or the review of, the submitted manuscript.

Declaration of Competing Interest

The author(s) declared no potential conflicts of interest with respect to the research, authorship, and/or publication of this article.

Acknowledgement

The authors would like to acknowledge the supports from Natural Science Foundation of China (Grand No. 52108083, 62072324), National Key R&D Program of China (Grand No. 2020YFC2006602), Natural Science Foundation of Jiangsu Province of China (Grand No. BK20190942, BE2020026).

References

Astrand, P. O., & Rodahl, K. (1977). *Textbook of Work Physiology-Physiological Bases of Exercise, Neuromuscular Function* (2nd Edition). New York: McGraw-Hill Book Company. McGraw-Hill.

Berlanga, F., Liu, L., Nielsen, P. V., Jensen, R. L., Costa, A., Olmedo, I., & Ruiz de Adana, M. (2020). Influence of the geometry of the airways on the characterization of exhalation flows. Comparison between two different airway complexity levels performing two different breathing functions. *Sustainable Cities and Society, 53*, Article 101874. https://doi.org/10.1016/j.scs.2019.101874

Blocken, B., van Druenen, T., van Hooff, T., Verstappen, P. A., Marchal, T., & Marr, L. C. (2020). Can indoor sports centers be allowed to re-open during the COVID-19 pandemic based on a certificate of equivalence? *Building and Environment, 180*, Article 107022.

Blocken, B., van Druenen, T., Ricci, A., Kang, L., van Hooff, T., Qin, P., Xia, L., Ruiz, C. A., Arts, J. H., Diepens, J. F. L., Maas, G. A., Gillmeier, S. G., Vos, S. B., & Brombacher, A. C. (2021). Ventilation and air cleaning to limit aerosol particle concentrations in a gym during the COVID-19 pandemic. *Building and Environment*. https://doi.org/10.1016/j.buildenv.2021.107659, 193(February).

Buonanno, G., Stabile, L., & Morawska, L. (2020). Estimation of airborne viral emission: Quanta emission rate of SARS-CoV-2 for infection risk assessment. *Environment International*. https://doi.org/10.1016/j.envint.2020.105794, 141(May).

Cakyova, K., Figueiredo, A., Oliveira, R., Rebelo, F., Vicente, R., & Fokaides, P. (2021). Simulation of passive ventilation strategies towards indoor CO2 concentration reduction for passive houses. *Journal of Building Engineering, 43*(August), Article 103108. https://doi.org/10.1016/j.jobe.2021.103108

Calvaresi, A., Arnesano, M., Pietroni, F., & Revel, G. M. (2018). Measuring metabolic rate to improve comfort management in buildings. *Environmental Engineering and Management Journal, 17*(10), 2287–2296. https://doi.org/10.30638/eemj.2018.227

Cao, S. J., Feng, Z., Wang, J., Ren, C., Zhu, H. C., Chen, C., & Mei, J. (2021). Ergonomics-oriented operation, maintenance and control of indoor air environment for public buildings. *Chinese Science Bulletin*. https://doi.org/10.1360/TB-2021-1024

Cao, S. J., Yu, C. W., & Luo, X. (2020a). Heating, ventilating and air conditioning system and environmental control for wellbeing. *Indoor and Built Environment, 29*(9), 1191–1194. https://doi.org/10.1177/1420326X20951967

Cao, S. J., Yu, C. W., & Luo, X. (2020b). New and emerging building ventilation technologies. *Indoor and Built Environment, 29*(4), 483–484. https://doi.org/10.1177/1420326X20909092

Chun, S. Y., Lee, C. S., & Jang, J. S. (2015). Real-time smart lighting control using human motion tracking from depth camera. *Journal of Real-Time Image Processing, 10*(4), 805–820. https://doi.org/10.1007/s11554-014-0414-1

China Academy of Building Science. (2016). *Design Code for Heating, Ventilation and Air Conditioning in Civil Buildings (GB50736-2016)*. Beijing, China.

Ding, J., Yu, C. W., & Cao, S. J. (2020). HVAC systems for environmental control to minimize the COVID-19 infection. *Indoor and Built Environment, 29*(9), 1195–1201. https://doi.org/10.1177/1420326X20951968

Enis Cetin, A., Ozturk, Y., Hanosh, O., & Ansari, R. (2021). Review of signal processing applications of Pyroelectric Infrared (PIR) sensors with a focus on respiration rate and heart rate detection. *Digital Signal Processing: A Review Journal, 119*. https://doi.org/10.1016/j.dsp.2021.103247

Feng, Z., Cao, S. J., & Haghighat, F. (2021). Removal of SARS-CoV-2 using UV+Filter in built environment. *Sustainable Cities and Society, 74*, Article 103226. https://doi.org/10.1016/j.scs.2021.103226

Feng, Z., Cao, S. J., Wang, J., Kumar, P., & Haghighat, F. (2021). Indoor airborne disinfection with electrostatic disinfector (ESD): Numerical simulations of ESD performance and reduction of computing time. *Building and Environment, 200*, Article 107956. https://doi.org/10.1016/j.buildenv.2021.107956

Guo, B. H. W., Zou, Y., Fang, Y., Goh, Y. M., & Zou, P. X. W. (2021). Computer vision technologies for safety science and management in construction: A critical review and future research directions. *Safety Science, 135*. https://doi.org/10.1016/j.ssci.2020.105130 (December 2020).

Hasan, M. H., Alsaleem, F., & Rafaie, M. (2016). Sensitivity study for the PMV thermal comfort model and the use of wearable devices biometric data for metabolic rate estimation. *Building and Environment, 110*, 173–183. https://doi.org/10.1016/j.buildenv.2016.10.007

Huang, Q., & Hao, K. (2020). Development of cnn-based visual recognition air conditioner for smart buildings. *Journal of Information Technology in Construction, 25*, 361–373. https://doi.org/10.36680/j.itcon.2020.021

Ibrahim, A. M., & Hassanain, M. A. (2022). Assessment of COVID-19 precautionary measures in sports facilities: A case study on a health club in Saudi Arabia. *Journal of Building Engineering, 46*, Article 103662. https://doi.org/10.1016/j.jobe.2021.103662

Jang, S., Han, S. H., & Rhee, J. Y. (2020). Cluster of Coronavirus disease associated with fitness dance classes, South Korea. *Emerging Infectious Diseases, 26*(8), 1917–1920. https://doi.org/10.3201/eid2608.200633

Jin, M., Bekiaris-Liberis, N., Weekly, K., Spanos, C. J., & Bayen, A. M. (2018). Occupancy Detection via Environmental Sensing. *IEEE Transactions on Automation Science and Engineering, 15*(2), 443–455. https://doi.org/10.1109/TASE.2016.2619720

Kang, D. W., Choi, J. S., Lee, J. W., & Tack, G. R. (2012). Prediction of Energy Consumption According to Physical Activity Intensity in Daily Life Using Accelerometer. *International Journal of Precision Engineering and Manufacturing, 13*(4), 617–621. https://doi.org/10.1007/s12541-012-0079-2

Kapalo, P., Vojtasko, L., Vasilisin, D., Domniţa, F., Bacoţiu, C., Kandrac, R., & Batorova, M. (2021). Investigation of the influence of the level of physical activity on the air exchange requirements for a gym. *Building and Environment, 204*(July). https://doi.org/10.1016/j.buildenv.2021.108123.

Kong, X., Guo, C., Lin, Z., Duan, S., He, J., Ren, Y., & Ren, J. (2021). Experimental study on the control effect of different ventilation systems on fine particles in a simulated hospital ward. *Sustainable Cities and Society, 73*(June). https://doi.org/10.1016/j.scs.2021.103102

Mokhtari, R., & Jahangir, M. H. (2021). The effect of occupant distribution on energy consumption and COVID-19 infection in buildings: A case study of university building. *Building and Environment, 190*. https://doi.org/10.1016/j.buildenv.2020.107561 (October 2020).

Monge-Barrio, A., Bes-Rastrollo, M., Dorregaray-Oyaregui, S., González-Martínez, P., Martin-Calvo, N., López-Hernández, D., Arriazu-Ramos, A., & Sánchez-Ostiz, A. (2022). Encouraging natural ventilation to improve indoor environmental conditions at schools. Case studies in the north of Spain before and during COVID. *Energy and Buildings, 254*, Article 111567. https://doi.org/10.1016/j.enbuild.2021.111567

Morawska, L., Allen, J., Bahnfleth, W., Bluyssen, P. M., Boerstra, A., Buonanno, G., Cao, J., Dancer, S. J., Floto, A., Franchimon, F., Greenhalgh, T., Haworth, C., Hogeling, J., Isaxon, C., Jimenez, J. L., Kurnitski, J., Li, Y., Loomans, M., Marks, G., & Yao, M. (2021). A paradigm shift to combat indoor respiratory infection. *Science, 372*(6543), 689–691. https://doi.org/10.1126/science.abg2025

Morawska, L., Tang, J. W., Bahnfleth, W., Bluyssen, P. M., Boerstra, A., Buonanno, G., Cao, J., Dancer, S., Floto, A., Franchimon, F., Haworth, C., Hogeling, J., Isaxon, C., Jimenez, J. L., Kurnitski, J., Li, Y., Loomans, M., Marks, G., Marr, L. C., & Yao, M. (2020). How can airborne transmission of COVID-19 indoors be minimised? *Environment International, 142*(April). https://doi.org/10.1016/j.envint.2020.105832

Na, H., Choi, H., & Kim, T. (2020). Metabolic rate estimation method using image deep learning. *Building Simulation, 13*(5), 1077–1093. https://doi.org/10.1007/s12273-020-0707-1

Na, H. S., Choi, J. H., Kim, H. S., & Kim, T. (2019). Development of a human metabolic rate prediction model based on the use of Kinect-camera generated visual data-driven approaches. *Building and Environment, 160*, Article 106216. https://doi.org/10.1016/j.buildenv.2019.106216 (December 2018).

Nagarajan, S. M., Deverajan, G. G., Chatterjee, P., Alnumay, W., & Ghosh, U. (2021). Effective task scheduling algorithm with deep learning for Internet of Health Things (IoHT) in sustainable smart cities. *Sustainable Cities and Society, 71*(January), Article 102945. https://doi.org/10.1016/j.scs.2021.102945

Nishi, Y. (1981). *Chapter 2: Measurement of Thermal Balance of Man* (pp. 29–39). Bioengineering, Thermal Physiology and Comfort.

Noorimotlagh, Z., Jaafarzadeh, N., Martínez, S. S., & Mirzaee, S. A. (2021). A systematic review of possible airborne transmission of the COVID-19 virus (SARS-CoV-2) in the indoor air environment. *Environmental Research, 193*. https://doi.org/10.1016/j.envres.2020.110612 (December 2020).

Pan, S., Liu, Y., Xie, L., Wang, X., Yuan, Y., & Jia, X. (2020). A thermal comfort field study on subway passengers during air-conditioning season in Beijing. *Sustainable Cities and Society, 61*, Article 102218. https://doi.org/10.1016/j.scs.2020.102218

Panaras, G., Markogiannaki, M., Tolis, E. I., Sakellaris, Y., & Bartzis, J. G. (2018). Experimental and theoretical investigation of air exchange rate of an indoor aquatic center. *Sustainable Cities and Society, 39*, 126–134. https://doi.org/10.1016/j.scs.2018.02.012

Pang, Z., Chen, Y., Zhang, J., O'Neill, Z., Cheng, H., & Dong, B. (2020). Nationwide HVAC energy-saving potential quantification for office buildings with occupant-centric controls in various climates. *Applied Energy, 279*(May). https://doi.org/10.1016/j.apenergy.2020.115727

Ren, C., & Cao, S. J. (2020). Implementation and visualization of artificial intelligent ventilation control system using fast prediction models and limited monitoring data. *Sustainable Cities and Society, 52*, Article 101860. https://doi.org/10.1016/j.scs.2019.101860

Shan, X., Luo, N., Sun, K., Hong, T., Lee, Y. K., & Lu, W. Z. (2020). Coupling CFD and building energy modelling to optimize the operation of a large open office space for occupant comfort. *Sustainable Cities and Society, 60*, Article 102257. https://doi.org/10.1016/j.scs.2020.102257

Shi, Y., Yan, Z., Li, C., & Li, C. (2021). Energy consumption and building layouts of public hospital buildings: A survey of 30 buildings in the cold region of China. *Sustainable Cities and Society, 74*, Article 103247. https://doi.org/10.1016/j.scs.2021.103247

Shin, M. S., Rhee, K. N., Lee, E. T., & Jung, G. J. (2018). Performance evaluation of CO2-based ventilation control to reduce CO2 concentration and condensation risk in residential buildings. *Building and Environment, 142*(March), 451–463. https://doi.org/10.1016/j.buildenv.2018.06.042

Simpson, R. J., Kunz, H., Agha, N., & Graff, R. (2015). Exercise and the Regulation of Immune Functions. *Progress in Molecular Biology and Translational Science*. https://doi.org/10.1016/bs.pmbts.2015.08.001

Srivastava, S., Zhao, X., Manay, A., & Chen, Q. (2021). Effective ventilation and air disinfection system for reducing coronavirus disease 2019 (COVID-19) infection risk in office buildings. *Sustainable Cities and Society, 75*(July), Article 103408. https://doi.org/10.1016/j.scs.2021.103408

Sun, C., & Zhai, Z. (2020). The efficacy of social distance and ventilation effectiveness in preventing COVID-19 transmission. *Sustainable Cities and Society, 62*(June), Article 102390. https://doi.org/10.1016/j.scs.2020.102390

Sun, K., Zhao, Q., Zhang, Z., & Hu, X. (2022). Indoor occupancy measurement by the fusion of motion detection and static estimation. *Energy and Buildings, 254*, Article 111593. https://doi.org/10.1016/j.enbuild.2021.111593

Wang, J., Huang, J., Feng, Z., Cao, S. J., & Haghighat, F. (2021). Occupant-density-detection based energy efficient ventilation system: Prevention of infection transmission. *Energy and Buildings, 240*, Article 110883. https://doi.org/10.1016/j.enbuild.2021.110883

Wang, J., Tse, N. C. F., & Chan, J. Y. C. (2019). Wi-Fi based occupancy detection in a complex indoor space under discontinuous wireless communication: A robust filtering based on event-triggered updating. *Building and Environment, 151*(January), 228–239. https://doi.org/10.1016/j.buildenv.2019.01.043

Wang, J., Tse, N. C. F., Poon, T. Y., & Chan, J. Y. C. (2018). A practical multi-sensor cooling demand estimation approach based on visual, indoor and outdoor information sensing. *Sensors (Switzerland), 18*(11). https://doi.org/10.3390/s18113591

World Health Organization (WHO). WHO Coronavirus (COVID-19) Dashboard, https://covid19.who.int/ (accessed on January 21, 2022).

Yang, L., Zhao, S., Gao, S., Zhang, H., Arens, E., & Zhai, Y. (2021). Gender differences in metabolic rates and thermal comfort in sedentary young males and females at various temperatures. *Energy and Buildings, 251*, 36–38. https://doi.org/10.1016/j.enbuild.2021.111360

Zhao, J., Xiao, Y., Liu, H., Lv, Y., & Liu, J. (2021). Indoor-outdoor relationship of PM2.5 mass concentrations in severe cold regions based on a coupled canopy model. *Sustainable Cities and Society, 75*, Article 103320. https://doi.org/10.1016/j.scs.2021.103320